Large-Scale Precipitation and Outgoing Longwave Radiation from INSAT-1B during the 1986 Southwest Monsoon Season

PHILLIP A. ARKIN

Climate Analysis Center, NMC/NWS/NOAA, Washington, D.C.

A. V. R. KRISHNA RAO AND R. R. KELKAR

India Meteorological Department, New Delhi, India

(Manuscript received 29 June 1988, in final form 4 January 1989)

ABSTRACT

Areally averaged precipitation and broadband outgoing longwave radiation (OLR) have been estimated from infrared window channel observations from INSAT-1B, the Indian geostationary satellite, for the period June–September 1986. The estimation techniques used were identical with those contained in previously published work using GOES (for precipitation) and NOAA (for OLR) satellite data. The fields of estimated monthly mean precipitation and OLR are quite similar, with regions of low flux corresponding to areas of heavy precipitation. Two bands of heavy rainfall were found, one near the equator, possibly associated with the Intertropical Convergence Zone, and another extending northwestward from Indonesia through the Bay of Bengal and over India. This latter feature exhibited a pronounced southeastward retreat during the course of the season. The rainfall estimates are reasonably consistent in both distribution and magnitude over India with climatological mean fields derived from rain gauge measurements. The OLR is similar in distribution but is about 5–10 W m^{-2} less in magnitude over land than that derived from observations from NOAA polar-orbiting satellites. Comparisons between weekly estimated rainfall and station rainfall observations show that the quantitative relationships between cloudiness and rainfall found in previous work are confirmed over most of India. An area along the west coast where orographic rainfall is important exhibits much higher correlations when a cloud top temperature of 265 or 270 K is used as the upper threshold for precipitation instead of 235 K.

1. Introduction

Data from the Indian geosynchronous satellite IN-SAT-1B promise to provide a wealth of information concerning the temporal and spatial variability of clouds and surface temperatures over the Indian subcontinent and Indian Ocean. Applications such as analysis of significant synoptic features began shortly after its launch (October 1983), and cloud motion vector extraction commenced in 1984 (Kelkar and Khanna 1986); the routine operational production of fields of statistics or derived data, however, has only begun recently. In this paper we shall describe two such efforts and present some early results of this work. Both the projects described here were developed under the Indo-U.S. Science and Technology Initiative, as a part of the effort to understand the interannual variability of the Indian monsoon.

Measurements of rainfall on various time and space scales are critical to understanding the Indian summer monsoon. While most areas of India have enough rain

Corresponding author address: Dr. Phillip A. Arkin, Climate Analysis Center/NMC/NWS/NOAA, W/MNC52, WWB, Washington, DC 20233.

gauges to obtain adequate estimates of areally averaged rainfall, some do not, and the nearby ocean regions are essentially unsampled. Estimates of large scale rainfall from INSAT-1B will permit the determination of the relationship of monsoon rainfall over India to that over the Indian Ocean. It will also fill the gap between areas viewed by the Japanese and European satellites and make possible the derivation of rainfall estimates for the entire tropical belt. We will describe an attempt to use the bulk statistics of IR cloud top temperatures to estimate areally averaged rainfall for a grid of 2.5° latitude × 2.5° longitude areas. The initial approach is identical with one which has been used to obtain such estimates from GOES since December 1981 (Arkin and Meisner 1987).

Another activity described here is the estimation of fields of broadband outgoing longwave radiation (OLR) from INSAT-1B 10.5–12.5 μm infrared (IR) data. Fields of OLR have been derived for many years from the NOAA polar-orbiting satellites and have proven very useful in studies of the radiation balance (Gruber and Winston 1978; Gruber and Krueger 1984), and in defining spatial and temporal variability in tropical convective activity (Liebmann and Hartmann 1982). It has also been suggested that variations of the surface

temperature of the Tibetan Plateau, and hence the OLR, may be important in determining the timing and intensity of the summer monsoon (Kelkar et al. 1985; Chen et al. 1985). In this region, where the diurnal cycle in surface temperature may be large, OLR measurements from INSAT-1B should be superior to those from NOAA, due to the more frequent sampling possible (up to 8 day^{-1} rather than 2–4 day^{-1}).

In section 2 we present descriptions of the procedures used to derive estimates of rainfall and OLR, together with reviews of the relevant literature. Section 3 contains a description of the monthly variability in estimated rainfall and OLR through the 1986 summer monsoon season. In section 4 we compare estimates of rain from INSAT-1B with those derived from rain gauge measurements over India, while section 5 summarizes and concludes.

2. Derivation

a. Precipitation

Arkin (1979) and Richards and Arkin (1981) used data from the GARP Atlantic Tropical Experiment (GATE) to show that for appropriate spatial scales (1.5° × 1.5° or 2.5° × 2.5°) the fraction of an area covered by cold (<235 K) cloud in hourly imagery was highly correlated (>0.7) with areally averaged hourly rainfall accumulations in the same area. Threshold temperatures ranging from 225 K to 250 K gave similar results, while temporal averaging over periods up to 24 h improved the correlations to as high as 0.9. Arkin and Meisner (1987) computed rainfall estimates from GOES data for the western hemisphere tropics and subtropics for the period December 1981 to November 1984. They found good correspondence with observed rainfall in most regions on monthly and seasonal time scales.

The rainfall estimation technique used in these works is an extremely simple indirect scheme (Arkin and Meisner 1987). Such techniques are so named because they use observations of quantities other than raindrops. In many such schemes, the process followed (although often only implicitly) is to determine, for some small region (usually one picture element, or "pixel"), a rain rate and the probability that rain is falling. The product of the probability, the rain rate and a duration yields estimated precipitation for a time period. This estimate can then be accumulated and/or averaged to the desired scales. In the technique used by Arkin and Meisner (1987), and in this paper, the probability of rainfall is a step function of equivalent blackbody brightness temperature (EBBT) for each pixel and the rain rate is a constant. The probability is 0 for EBBT > 235 K and 1 for lower temperatures. This is approximately the EBBT for which maximum correlations were found by Richards and Arkin (1981), while the constant rain rate used (71.2 mm day^{-1}) is that derived from the regression for which they found the

highest correlation. The algorithm has been used without change for the INSAT-1B estimates described here. To allow its application, along with the testing of the effect of changing temperature thresholds, histograms of EBBT were computed from three-hourly interval imagery for weekly and monthly periods for each 2.5° latitude × 2.5° longitude area from 35°N–20°S and from 40°E–100°E using the classes given by Arkin and Meisner (1987). The size of the INSAT-1B IR pixel is 11 × 11 km at the subsatellite point.

In the present work, the transformation from satellite coordinates to earth coordinates was performed a single time for every pixel, and a look-up table identifying the geographic positions was created. This is possible (and desirable, since the transformation is computationally rather expensive) because INSAT-1B is three-axis stable, and hence a given line and pixel should in principle correspond to a fixed earth location. In practice, however, position error of the order of a pixel may occur.

b. OLR

Operational estimation of broadband outgoing longwave radiation (OLR) from polar-orbiting NOAA satellites commenced in June 1974 (Gruber and Krueger 1984) and has continued since then. The NOAA global OLR dataset, in spite of alterations in satellite radiometer characteristics and equator-crossing times, has been continuous enough to be brought out in atlas form (Janowiak et al. 1985; Gruber et al. 1986).

These estimates of OLR are made by means of a regression equation relating OLR and the actual narrowband radiance measurement of a particular satellite radiometer. In terms of temperatures, and for a nadir view, this regression is assumed to take the form

$$T_f = T_B(a + bT_B) \qquad (1)$$

where T_f is the blackbody flux temperature, T_B is the narrow channel EBBT, both in K, and a, b are constants (Ohring et al. 1984). OLR is then computed as σT_f^4, where σ is the Stefan–Boltzmann constant.

Because the values of the regression coefficients differ from one radiometer to another, a and b were evaluated for the spectral response characteristics of the INSAT-1B VHRR in the 10.5–12.5 μm IR window channel (R. Ellingson, private communication). For zero zenith angle, $a = 1.1889$ and $b = -0.000989$ K^{-1}; both decrease in magnitude with increasing zenith angle.

Given the flux temperature of each individual pixel in an INSAT-1B image, the mean OLR of a 2.5° × 2.5° area can be derived either by computing OLR for each pixel and then averaging all the values within the box, or by computing a mean temperature for the area and deriving the corresponding OLR value. The difference between these depends on the second to fourth spatial moments of T and was shown to be at the most 1–2 W m^{-2} in the data used here. The simpler approach

of computing OLR from the area–mean T was used in the present study.

3. QPE and OLR variability during June–September 1986

The computation of histograms and means of EBBT from full-resolution INSAT-1B imagery, and hence the capability to calculate quantitative precipitation estimates (QPE) and OLR in the manner described in section 2, began on 1 June 1986. In this section we shall present and discuss the QPE and OLR for the months (June–September) of the summer monsoon season of 1986. While our primary intent is to provide an illustration of the application of these techniques to INSAT-1B data, the results also provide some useful information not previously available on the spatial and temporal variability of these climatically significant parameters.

a. QPE

We begin with a description of monthly QPE during this season. During June, maxima in estimated rainfall are seen in the Bay of Bengal and the Arabian Sea, with the center of the latter near the west coast of southern India (Fig. 1a). Peak values of more than 700 mm in the former and 600 mm in the latter are seen, with a secondary maximum of >400 mm found over India in a belt of QPE > 200 mm which connects the two oceanic maxima. QPE > 100 mm covers essentially all of the oceanic area east of 55°E and north of 10°S, except for the northernmost part of the Arabian Sea. QPE > 100 mm covers most of the subcontinent except for the extreme north and west. A very pronounced minimum is seen over Iran, the Arabian Peninsula and the Persian Gulf, with another small area of minimum values located over Sri Lanka. Other regions of low QPE are seen in the southern Indian Ocean and near Africa. No QPE maximum which can be identified with an equatorial convergence zone is seen in this month.

During July (Fig. 1b), QPE decreased to near 0 over the western Arabian Sea and to 200 mm off the west coast of India. A maximum of >600 mm remains over the Bay of Bengal, with an area of QPE > 400 mm extending westward across central India. QPE > 100 mm covers most of India, with peak values of >600 mm south of New Delhi. A minimum is once again observed over Sri Lanka and in the southern Indian Ocean, while there does appear to be an area of maximum QPE (>200 mm) centered near the equator east of about 70°E.
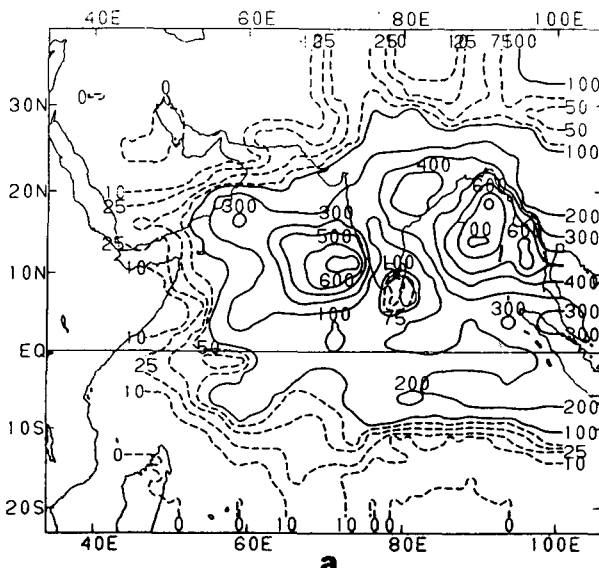
During August (Fig. 1c), features west of 70°E remain similar to those found in July, with very low values over most of the Arabian Sea, the Arabian Peninsula and Iran. The maximum over the Bay of Bengal has shifted towards the southeast and decreased somewhat in amplitude, with peak values between 500–600 mm. An extension towards the northwest remains but

is not so pronounced as in July. Maximum values over land are 300–400 mm at the head of the Bay of Bengal and along the coast of Andhra Pradesh. The minimum near Sri Lanka has expanded and now covers the southern tip of India, as well as extending well into the Bay of Bengal. The Indian Ocean south of 10°S remains dry, while a rather clear QPE maximum, possibly associated with the Intertropical Convergence Zone (ITCZ), is seen to extend near and just south of the equator almost to 60°E. Maximum values in this feature exceed 400 mm.
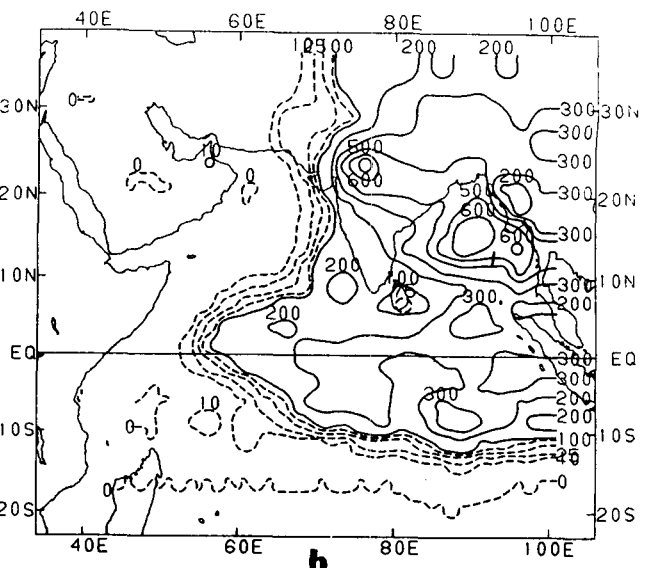
September (Fig. 1d) is quite dry by comparison with the preceding months except in the extreme east. QPE is <100 mm across an extensive portion of western and northwestern India and most of the Arabian Sea, along with all areas farther west. A poorly defined maximum extends up the Bay of Bengal and into Bangladesh, but with peak values of only 300 mm. This region appears to be an extension of a pair of near equatorial maxima (each > 400 mm) found near 100°E. Two small regions of QPE > 200 mm are found farther west, one near 70°E just north of the equator with the other along the southwest coast of India. The minimum over Sri Lanka retains the configuration observed during August, but with a slightly smaller areal extent.

The summation of these four months is shown in Fig. 1e to represent the total QPE for the monsoon season. Peak values of >2000 mm are observed over the central Bay of Bengal, with values > 1000 mm covering the head of the Bay and extending east–west across India. An area of QPE > 1000 mm extends westward and a bit northward from near 100°E just south of the equator to about 75°E. Another small area with QPE > 1000 mm is found just off the southwest coast of India. QPE is low across the Indian Ocean south of 12°S, and for all longitudes west of 60°E, as well as over the desert regions in the northwest part of the observed region. A minimum, with QPE values < 500 mm for the season, is centered on Sri Lanka.
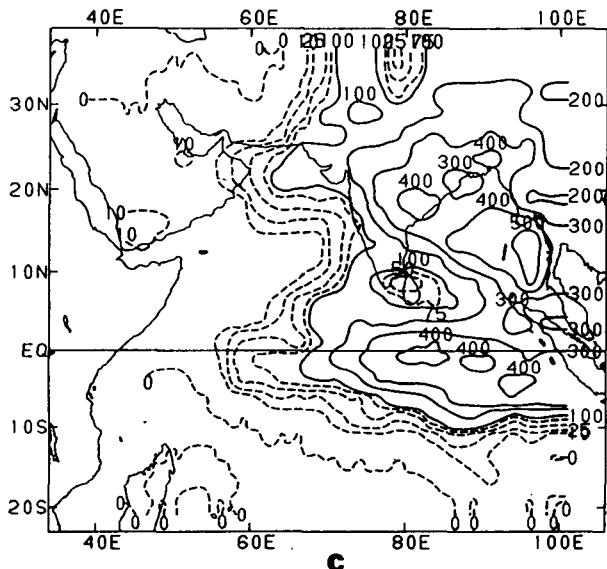
Verification of our QPE values is extremely difficult. In the section 4 we shall compare the values over India with observations, but we have no observations over ocean areas. For the Indian Ocean, no climatology derived from ship observations (such as those produced by Dorman and Bourke 1979, 1981 for the Atlantic and Pacific oceans) is available in the published literature. Jaeger (1976) has published maps of monthly and seasonal mean rainfall for the globe, but these are based on extrapolations of coastal and island station data. A comparison with his maps shows that both the distributions and amounts are qualitatively similar, although details differ substantially. Over India, long-term mean analyses based on station data are available (IMD 1981), and a comparison shows that several of the principal features found here are also present in the long-term mean. The minimum over Sri Lanka and southern India, the maximum at the head of the
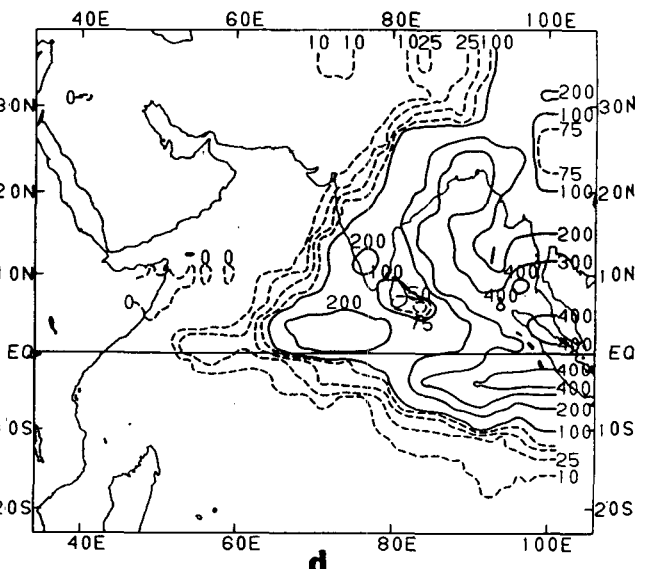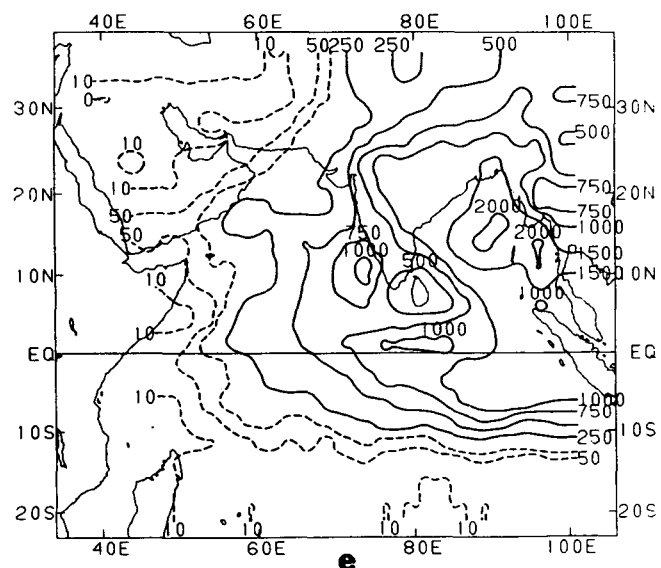
Bay of Bengal and extending northwestward, the general decrease towards northwest India and Pakistan, and a maximum off the southern part of the west coast all appear in both Fig. 1e and the climatological mean. Magnitudes appear to differ systematically along the west coast, where the QPE are quite low by comparison, and in the south where they are relatively high.

The most evident features shown by the maps of QPE appear to be a pair of bands of maxima extending from the eastern edge of the domain. One is located just south of the equator and extends westward to approximately 70°E. It has a slight northward trend in some months and is not continuous, but it is primarily zonal in orientation and may represent precipitation associated with the ITCZ. It becomes more clearly organized through the course of the season. The second extends northwestward from 100°E, just north of the equator across the Bay of Bengal and north central India. Peak values, except in September, were found in the Bay, and this feature is much broader in extent than the first. These two bands appear to be extending from a common origin near the equator, but one which is east of the domain of this study. Inspection of maps of mean OLR from the NOAA satellites (Janowiak et al. 1985) shows that maxima of convective activity of similar appearance originate from an area between Indochina and the Philippines. In June, the more northern of these bands appeared to extend across the subcontinent and to be linked to an area of high QPE covering much of the Arabian Sea. This area was not observed during later months.

There is an apparent tendency for QPE to decrease in most parts of the domain with the advance of the season. August, and particularly September, are quite dry across the Arabian Sea and northern and northwestern India by comparison with earlier months. The southeastward retreat of the region of high QPE across northern India would be consistent with an earlier than normal withdrawal of the monsoon in this year. Halpert and Ropelewski (1987) noted an early weakening in late August and a dry September, resulting in the poorest monsoon season since 1982.

b. OLR

Mean OLR for the months of June–September 1986 is shown in Fig. 2. The spatial patterns are very similar to those found in the monthly QPE maps (Fig. 1), with low values of OLR corresponding quite closely to high values of QPE. Areas with very low values of QPE correspond to regions of high OLR flux, but more detail is visible in the OLR distribution. The OLR responds

both to variations in cloudiness (both height and frequency of occurrence) and in surface temperature. Over the tropical oceans, because of the relatively stable surface temperature, OLR variations are due almost entirely to changes in the distribution of cloudiness, and are hence related to changes in precipitation. Over the Arabian Peninsula and Iran, clouds are much less frequent and surface temperatures are quite high, leading to high flux values.

The patterns of OLR shown here compare quite well to those contained in the OLR derived from observations from the NOAA polar-orbiting satellites for the same period (Halpert and Ropelewski 1987). The monthly pattern coefficients exceed 0.95. There does appear to be a small consistent difference, however, between the monthly means of the two analyses. The NOAA OLR appears to systematically exceed that calculated from INSAT-1B by 5–10 W m^{-2} over land, but is lower than or equal to the INSAT-1B OLR over cloudy ocean regions. While several possible causes for this difference exist, including different sampling of the diurnal cycle, the use of areal mean EBBT to calculate mean OLR, and differences in the spatial resolution of the radiometers, it does not seem possible to identify the actual cause from the information available. It is clear that further investigation of this difference is warranted.

4. Comparison of QPE for INSAT-1B and observed rainfall

Arkin and Meisner (1987), while acknowledging the difficulty of obtaining areally averaged rainfall from point observations, attempted to compare GOES-based estimates with estimates derived by arithmetically averaging all observations in a 2.5° area. Despite the obvious shortcomings in this process, they succeeded in obtaining some information about the spatial and temporal variability in the utility and accuracy of their estimates. Our objective in this section is similar: to understand the spatial variability in the skill of the QPE, and to determine whether there exist areas in India for which some alternative technique, perhaps the use of a different threshold temperature, might yield a superior rainfall estimate.

For our comparisons here, we use the weekly rainfall statistics collected by the India Meteorological Department for the subdivisions of India. There are 35 such regions (see Fig. 3 and Table 1); each is composed of a number of districts with various numbers of rain gauges in each district. Weekly subdivision rainfall is calculated by averaging all the area-weighted district

---

FIG. 1. Estimated rainfall for (a) June, (b) July, (c) August, and (d) September 1986. Solid contours at intervals of 100 mm; dashed contours at 25 mm intervals below 100 mm with an additional contour at 10 mm. (e) Estimated rainfall for the summer monsoon season of June–September 1986. Solid contours at intervals of 250 mm from 250–1000 mm and at 500 mm intervals above 1000 mm; dashed contours at 10, 50 and 100 mm.
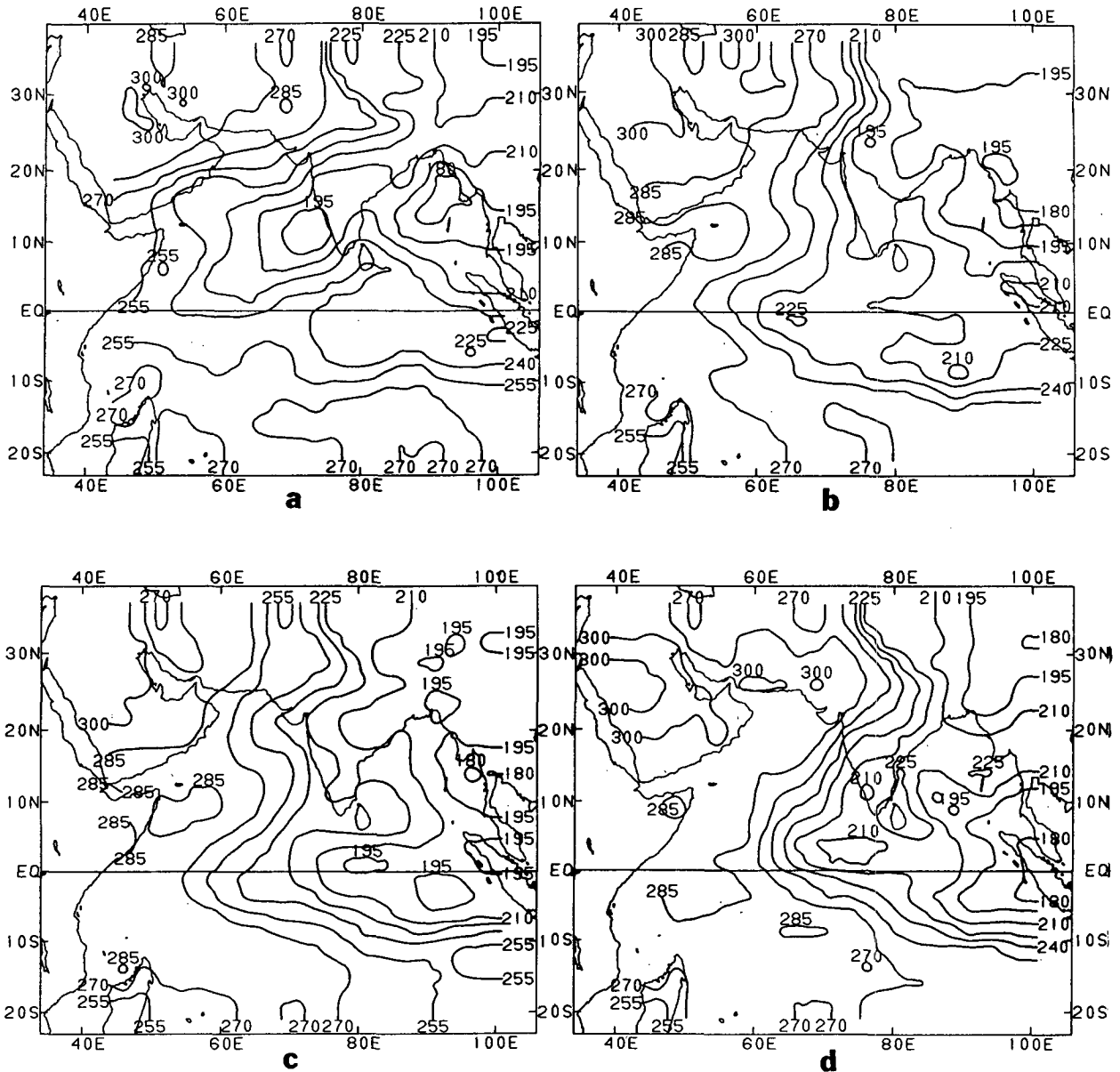
FIG. 2. Estimated outgoing longwave radiation for (a) June, (b) July, (c) August, and (d) September 1986. Contour interval of 15 W m^{-2}.

rainfalls. Rainfall for each district is the arithmetic average of the rain gauge observations for the week. Missing data are ignored. Arunachal Pradesh was not considered in the present study.

The QPE values were derived for each week during the period June–September 1986 for areas of 2.5° latitude/longitude for all of India. The subdivisions are based in general on political boundaries, with each representing all or a part of one of the states of the nation. In some cases, subdivision boundaries represent geographic features, such as the crest of the Western Ghats, because those features either form the boundary of a state or are otherwise convenient. QPE values for

each of the 2.5° areas contained either partially or completely within a subdivision are weighted according to their fractional coverage of the subdivision and then averaged.

We will compare the QPE as defined in section 2 with subdivision rainfall by computing correlation coefficients and linear regression parameters for each subdivision. We will also evaluate the effect of changing the temperature threshold for the QPE by performing the same calculations for thresholds of 190 K, 200 K and at each 5 K from 210–270 K, inclusive. The cloud amount using each of these thresholds has been used in the same algorithm as that given in section 2, so the
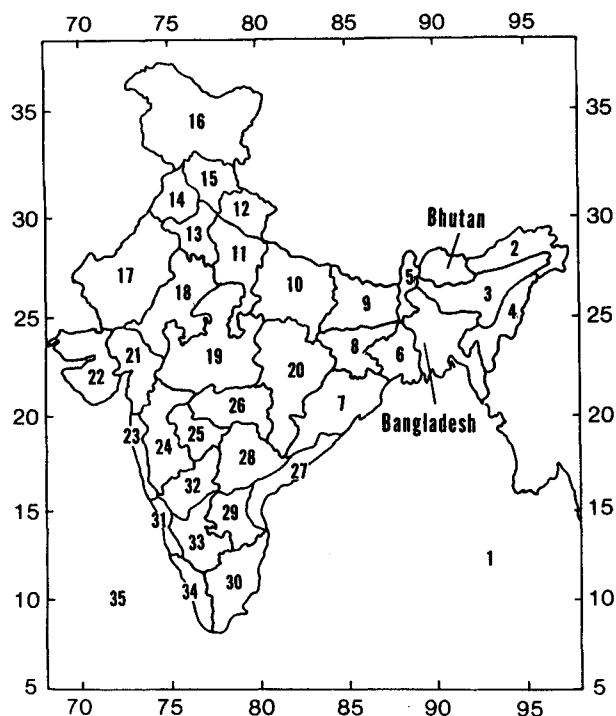
FIG. 3. Meteorological subdivisions of India from which rainfall data were obtained for use in this study. Numbers correspond to names in Table 1.

correlations; the four along the west coast from Konkan and Goa southward and the three along the north-western border from West Rajasthan to Punjab. Inspection of correlations calculated for other thresholds showed that values of 270 or 265 K yielded correlations of from 0.68–0.72 in the northwest and 0.86–0.91 along the southwest coast. For other subdivisions, correlations using these thresholds (Fig. 6 shows those for 265 K) were high but less than the peak values. Inspection of the threshold for which the maximum correlation was found, however, showed that all the west coast subdivisions from Gujarat southward had highest correlations for thresholds of 265 or 270 K. This was also true for the two subdivisions the least distance inland (Madhya Maharashtra and South Interior Karnataka), while the one next closest (North Interior Karnataka) had a correlation for a threshold of 270 K just 0.01 less than that for a threshold of 240 K. The only other subdivisions where maximum correlations were found for thresholds warmer than 255 K were the three along the northwestern border of India.

The result for the region near the west coast seems

quantitative estimates will not be meaningful, but the linear correlations for thresholds other than 235 K should provide some information.

Figure 4 shows estimated correlations by subdivision between the 17 weeks of rain gauge measurements and QPE based on a 235 K threshold. Because the lag 1 autocorrelations of the subdivision rainfall measurements during this period of 1986 are small, we may treat the 17 weekly values as serially independent. Thus, there is a 99% chance that the actual correlation is nonzero if the estimated correlation exceeds 0.575. Of the 34 subdivisions used here, 19 exhibited correlations of 0.69 or higher, and 12 were greater than or equal to 0.79. In these regions, it certainly appears that the relationship between the fractional coverage of cold cloud and rainfall is quite similar to that found by Arkin (1979) for the eastern tropical Atlantic. The slopes of the regression between QPE and subdivision rainfall (Fig. 5) show that, in subdivisions for which high correlations were found, the QPE generally overestimated the observed rainfall (a slope of 0.50 indicates that the QPE was double the observed). For many subdivisions, this overestimate was in the range of 10%–20%, but a few subdivisions had much larger overestimates even with high correlations. In a few subdivisions, including Himachal Pradesh, Jammu and Kashmir and Sub-Himalayan West Bengal, the slopes were greater than 1.00, indicating an underestimate by the satellite.

Two groups of subdivisions exhibited relatively low

TABLE 1. Meteorological subdivisions of India; numbers correspond to those in Fig. 3.

| No.	Name
1.	Andaman and Nicobar Islands
2.	Arunachal Pradesh
3.	Assam and Meghalaya
4.	Nagaland, Manipur and Tripura
5.	Sub.-Himalayan West Bengal and Sikkim
6.	Gangetic West Bengal
7.	Orissa
8.	Bihar Plateau
9.	Bihar Plains
10.	East Uttar Pradesh
11.	West Uttar Pradesh
12.	Uttar Pradesh Hills
13.	Haryana
14.	Punjab
15.	Himachal Pradesh
16.	Jammu and Kashmir
17.	West Rajasthan
18.	East Rajasthan
19.	West Madhya Pradesh
20.	East Madhya Pradesh
21.	Gujarat
22.	Saurashtra and Kutch
23.	Konkan and Goa
24.	Madhya Maharashtra
25.	Marathwada
26.	Vidarbha
27.	Coastal Andhra Pradesh
28.	Telangana
29.	Rayaleseema
30.	Tamil Nadu
31.	Coastal Karnataka
32.	North Interior Karnataka
33.	South Interior Karnataka
34.	Kerala
35.	Lakshadweep Island
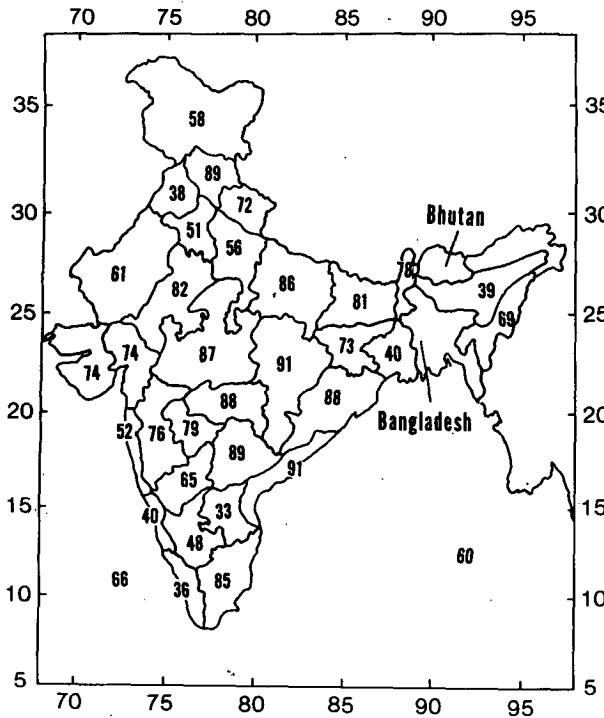
FIG. 4. Correlation (×100) between areally averaged weekly QPE and weekly subdivision rainfall for the monsoon season of 1986. Precise locations of subdivisions are given in Fig. 3.
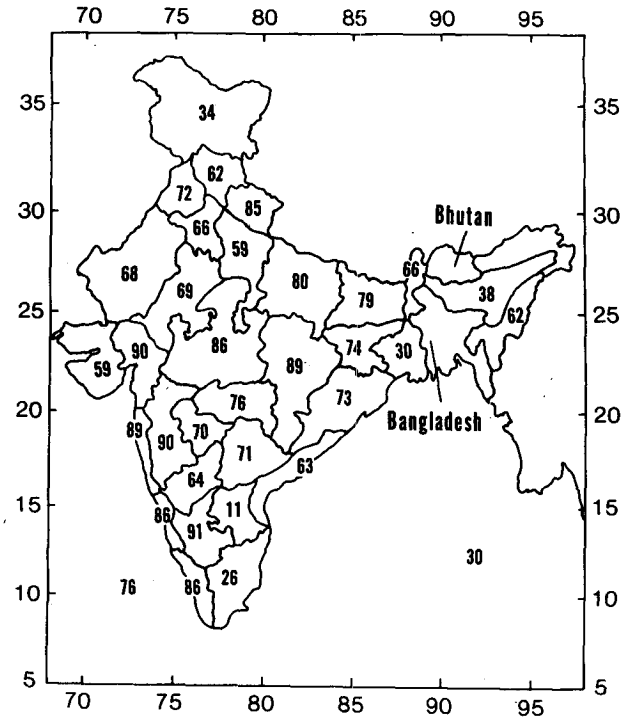

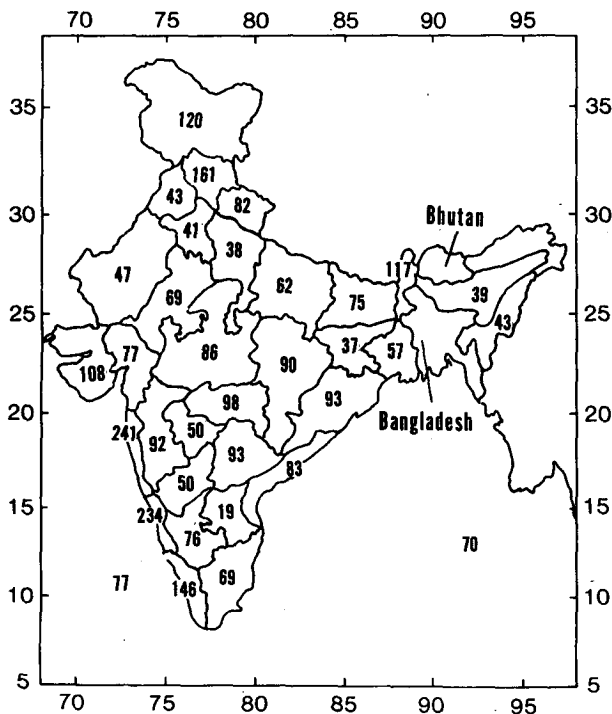FIG. 6. As in Fig. 4, except for the use of a threshold of 265 K to define the rainfall estimate.

FIG. 5. As in Fig. 4, except for the slope (×100) of the regression between weekly QPE and weekly subdivision rainfall.

rather easy to explain in terms of the rainfall physics which dominate the region. The southwest monsoon flow from the Arabian Sea blows against the Western Ghats, which run along the coast with peak heights of 1500–2600 m, and gives rise to substantial orographic rainfall. This orographic rainfall appears to be associated with clouds whose tops are relatively low and warm, and thus the amount of cloud which rises above the warmer thresholds is more closely related to the amount of precipitation than that which exceeds the colder thresholds. Unfortunately, the regression models developed by Richards and Arkin (1981) from GATE data cannot yield accurate quantitative rainfall estimates for such regions. The magnitude of the observed correlations indicates, however, that such estimates should be possible to obtain, given an appropriate set of detailed ground-based rainfall measurements.

It is not so easy to obtain an explanation for the group of subdivisions in northwest India. All three are in a relatively dry region, and the physics involved in the cloud–rainfall relationship there may be quite different from other areas. The scarcity of rainfall in this region, however, makes it difficult to assess the validity of our statistics there.

The other subdivisions for which peak correlations were relatively low were Gangetic West Bengal, Assam and Meghalaya, and Rayalaseema. In all three, peak

correlations ranged between 0.41–0.54 for thresholds ranging from 225–200 K. The first two of these border on Bangladesh, while the last is in southern India to the east of the Western Ghats.

5. Summary and conclusions

We have described the application of previously developed algorithms for the estimation of rainfall and outgoing longwave radiation to data from the Indian geostationary satellite INSAT-1B. The algorithm for rainfall is that based on statistical results from GATE data (Arkin 1979; Richards and Arkin 1981), and applied by Arkin and Meisner (1987) to GOES data. The algorithm for OLR conforms to one developed using IR window channel observations from the NOAA operational polar orbiting satellites (Gruber and Krueger 1984) but with numerical coefficients appropriate for the INSAT-1B radiometer. We have presented total estimated rainfall and mean OLR for each of the months of June–September during the summer monsoon season of 1986, and compared these results with published climatologies and data from the NOAA satellites. We also compared weekly rainfall estimates with subdivision rainfall over India, and examined the effect of varying the temperature threshold between 190–270 K.

The sequences of QPE and OLR maps indicate that areas of deep convection during this season were organized into two principal regions, both extending westward from the eastern border of the domain (near 100°E). One exhibits a nearly zonal orientation near and south of the equator and extends westward to between 60°–70°E, while the other extends northwestward across the Bay of Bengal and into northwest India. During June, this band was linked to an area of high QPE in the Arabian Sea. Dry conditions were found near Sri Lanka, in the south and west Indian Ocean, over the desert regions in the Arabian Peninsula and Iran, and over most of the Arabian Sea after June. The clearest impression left by the sequence of maps is one of a general southeastward retreat of the areas of rainfall and low OLR through the season. The comparisons of QPE with climatological rainfall indicate that the estimates are of plausible magnitude and that the principal climatological features do appear to be represented. The OLR from INSAT-1B is highly correlated with that derived from NOAA satellite observations, but appears to differ by 5–10 W m^{-2} over land areas.

A comparison of QPE from INSAT-1B with weekly rainfall for the subdivisions of India shows that very high correlations were found in about two-thirds of the 34 regions, with regression slopes of slightly less than one, indicating an overestimate by the satellite algorithm of 10%–20%. Two groups of regions were found where correlations were much higher if warmer thresholds of 270 or 265 K were used, one along the west

coast and the other over northwest India. Three subdivisions had rather low correlations regardless of the threshold tried.

The comparison between the QPE and subdivision rainfall, in general, confirms the results of Arkin (1979) for the GATE region, in that the correlation between fractional cloud cover of relatively large areas and observed rainfall is observed to be quite high for a broad range of threshold temperatures. The findings of Arkin and Meisner (1987) regarding the tendency for the estimation algorithm developed from GATE data to overestimate over continental interiors was confirmed as well. The time scale addressed here was intermediate between those two studies. These results also appear to indicate that the potential to estimate orographic rainfall in at least some regions with a very simple satellite-based algorithm may exist.

This study has shown that both QPE and OLR can be derived from digital data from the INSAT-1B geostationary satellite in near real-time and with rather modest effort. These estimates certainly appear to provide sufficient information to make them useful for certain applications. A few examples of such applications include: (i) real-time monitoring of large-scale rainfall over the Indian subcontinent, both as preliminary and supplemental information to the available gauge network; (ii) providing a means by which oceanic rainfall, especially in the Arabian Sea, Bay of Bengal and equatorial Indian Ocean, can be quantitatively related to rainfall over the subcontinent; and (iii) monitoring of radiation budget parameters, potentially including albedo as well as OLR, over the subcontinent, the arid region to the north and west, and the Tibetan Plateau, with much superior sampling of the diurnal cycle compared to currently available data.

REFERENCES

Arkin, P. A., 1979: The relationship between fractional coverage of high cloud and rainfall accumulations during GATE over the *B*-scale array. *Mon. Wea. Rev.*, **107**, 1382–1387.
——, and B. N. Meisner, 1987: The relationship between large-scale convective rainfall and cold cloud over the western hemisphere during 1982–84. *Mon. Wea. Rev.*, **115**, 51–74.

Chen, L., E. R. Reiter and Z. Feng, 1985: The atmospheric heat source over the Tibetan plateau: May–August 1979. *Mon. Wea. Rev.,* **113,** 1771–1790.

Dorman, C. E., and R. H. Bourke, 1979: Precipitation over the Pacific Ocean, 30°S to 60°S. *Mon. Wea. Rev.,* **107,** 896–910.

——, and ——, 1981: Precipitation over the Atlantic Ocean, 30°S to 70°N. *Mon. Wea. Rev.,* **109,** 554–563.

Gruber, A., and J. S. Winston, 1978: Earth–atmosphere radiative heating based on NOAA scanning radiometer measurements. *Bull. Amer. Meteor. Soc.,* **59,** 1570–1573.

——, and A. F. Krueger, 1984: The status of the NOAA outgoing longwave radiation data set. *Bull. Amer. Meteor. Soc.,* **65,** 958–962.

——, M. Varnadore, P. A. Arkin and J. S. Winston, 1986: Monthly and seasonal mean outgoing longwave radiation and anomalies. *NOAA Tech. Rep. NESDIS-26,* U.S. Dept. of Commerce, NOAA/NESDIS, 5 pp. + figures [NTIS No. PB87-160545-AS].

Halpert, M. S., and C. F. Ropelewski, 1987: The global climate for June–August 1986: Dry conditions plague parts of the Northern Hemisphere. *Mon. Wea. Rev.,* **115,** 705–720.

India Meteorological Department, 1981: *Climatological Atlas of India, Part A (Rainfall),* 65 plates. [Available from India Meteorological Department, Lodi Road, New Delhi, 10003, India.]

Jaeger, L., 1976: Monatskarten des Niederschlags fur die ganze Erde.

Ber. Deutsch. Wetterdienstes, Nr. 139 (Band 18). Offenbach A.M., 33 pp. and plates. [Available from Deutscher Wetterdienst, Frankfurter Str. 135, Offenbach 6050, West Germany.]

Janowiak, J. E., A. F. Krueger, P. A. Arkin and A. Gruber, 1985: *Atlas of outgoing longwave radiation derived from NOAA satellite data.* NOAA Atlas No. 6, U.S. Dept. of Commerce, NOAA/NWS, Silver Spring, MD, 44 pp. [NTIS No. PB85-155455].

Kelkar, R. R., and P. N. Khanna, 1986: Automated extraction of cloud motion vectors from INSAT-1B imagery. *Mausam,* **37,** 495–500.

——, —— and S. Prasad, 1985: Infrared radiances over the Tibetan plateau as measured by INSAT-1A VHRR in an active monsoon situation. *Mausam,* **36,** 359–366.

Liebmann, B., and D. L. Hartmann, 1982: Annual variations of outgoing IR associated with tropical circulation changes during 1974–1978. *J. Atmos. Sci.,* **39,** 1153–1162.

Ohring, G., A. Gruber and R. G. Ellingson, 1984: Satellite determination of the relationship between total longwave radiation flux and infrared window radiance. *J. Climate Appl. Meteor.,* **23,** 416–425.

Richards, F., and P. Arkin, 1981: On the relationship between satellite-observed cloud cover and precipitation. *Mon. Wea. Rev.,* **109,** 1081–1093.